KARYA ILHAM PUBLISHING
CONNECTING MINDS, BRIDGING IDEAS, INSPIRING READERS

Malaysian Journal on Composites Science and Manufacturing

Journal homepage:
https://karyailham.com.my/index.php/mjcsm/index
ISSN: 2716-6945

Evaluation of Phosphate Removal by Activated Carbon from Palm Oil Mill Effluent (Pome) Sludge and Empty Fruit Bunch (EFB) Blend

Danish Akmal Jihat Ahmad[1], Nur Vida Aimar Faizai[1], Mohd Asmadi[1], Nur Hafizah Ab Hamid[1,*]

[1] Chemical Reaction Engineering Group (CREG), Faculty of Chemical and Energy Engineering, Universiti Teknologi Malaysia, 81310 Skudai, Johor, Malaysia

ARTICLE INFO

Article history:
Received 16 January 2026
Received in revised form 28 February 2026
Accepted 3 March 2026
Available online 31 March 2026

Keywords:

Palm Oil Mill Effluent (POME) sludge; Empty Fruit Bunch (EFB); phosphate adsorption; activated carbon

ABSTRACT

Adsorption using activated carbon has attracted considerable attention for phosphate removal from wastewater. In this study, Palm Oil Mill Effluent (POME) sludge and Empty Fruit Bunch (EFB) were blended and evaluated as precursor materials for activated carbon production. The efficiency of phosphate removal from aqueous solutions was assessed, and the physicochemical properties of the activated carbons prepared from different EFB-POME sludge compositions were characterised using Scanning Electron Microscopy coupled with Energy-Dispersive X-ray Spectroscopy (SEM–EDX) and Brunauer–Emmett–Teller (BET) surface area analysis. The biomasses were subjected to slow pyrolysis followed by chemical activation using calcium hydroxide ($Ca(OH)_2$). Batch adsorption experiments were conducted to evaluate adsorption performance under varying biomass compositions, contact times, and initial phosphate concentrations. Adsorption behaviour was further analysed using the Langmuir and the Freundlich isotherm models. BET analysis revealed specific surface areas of 9.404 m^2/g, 11.200 m^2/g, and 10.393 m^2/g for activated carbons derived from 100% EFB, the 60%EFB – 40%POME sludge and 100% sludge, respectively. SEM–EDX analysis indicated the presence of Ca^{2+} on the activated carbon surfaces, evidenced by 22 – 38 % Ca^{2+} detected. All activated carbons exhibited high phosphate adsorption performance, achieving a maximum adsorption capacity of 347.55 mg/g at an initial phosphate concentration of 350 mg/L. Isotherm analysis showed comparable adsorption performance among all samples with the highest Langmuir maximum adsorption capacity observed for 100% EFB (q_{max} = 332.652 mg/g), while the EFB–sludge composite exhibited the highest Freundlich constant (Kf = 393.236), indicating greater surface heterogeneity. Favourable adsorption behaviour was confirmed for all adsorbents, with n > 1 and strong model fitting (R^2 > 0.98 for the Langmuir model). Overall, this study demonstrates the successful valorisation of Palm Oil Mill Effluent (POME) sludge and Empty Fruit Bunch (EFB) as effective precursors for calcium-activated carbon in phosphate removal from wastewater, supporting waste-to-resource strategies and circular economy approaches in wastewater treatment.

* *Corresponding author.*
E-mail address: nurhafizah.abhamid@utm.my

https://doi.org/10.37934/mjcsm.19.1.8698

1. Introduction

The oil palm industry plays a crucial role in Malaysia's economic development. However, it also contributes significantly to environmental degradation through the discharge of nutrient-rich effluents into aquatic ecosystems. Excessive phosphate loading has been identified as a major cause of eutrophication, leading to ecological imbalance and deterioration of water quality in freshwater systems. It can also accelerate algal blooms and disrupt dissolved oxygen balance, affecting the aquatic biodiversity and water usability.

In several countries including Malaysia, nutrient pollution from agro-industrial activities remains a challenge due to the increasing production of palm oil and limited advanced wastewater treatment implementation [1-4]. Among various wastewater treatment technologies, adsorption has received considerable attention due to its simplicity, cost-effectiveness, and operational efficiency [5]. Activated carbon, in particular, has demonstrated excellent adsorption capacity due to its high surface area and porous structure. Compared to the conventional method of removing phosphate from wastewater such as chemical precipitation and biological nutrient removal, adsorption offers several advantages including reduced chemical consumption, lower sludge generation and operational flexibility [6]. These advantages make adsorption attractive for polishing treatment stages, where consistent phosphate removal is needed under varying influent conditions [5].

Activated carbon can be produced from several raw materials, with biomass being one of the most widely utilised precursors [7]. In addition, biomass-derived activated carbon has emerged as a sustainable alternative to commercial adsorbents, especially when derived from agricultural waste such as empty fruit bunches (EFB) and palm oil mill effluent (POME) sludge [8-10]. These materials are generated abundantly by the palm oil industry and possess favourable physicochemical properties for carbonisation and activation. Previous studies have shown that the activated carbon derived from EFB and POME sludge demonstrates promising adsorption performance for nutrient removal, including phosphate. This is mainly due to its porous structure and surface functionality developed during activation. The utilisation of this abundant waste can contribute to enhancing wastewater treatment efficiency and, most importantly waste valorisation and environmental sustainability [2].

Furthermore, the adsorption performance of activated carbon from these precursors has been reported by several researchers. Activated carbon using MgO is reported to have an adsorption performance of 99.1% [8-10]. Ca-modified biochar achieved an adsorption performance of more than 90% [11] and Fe/Ca co-embedded biochar up to 85 – 98% [12]. In addition, the adsorption performance of POME sludge-based activated carbon (AC) via physicochemical modification has been reported using calcium-based agents, achieving removal efficiencies of up to 90–98% [5]. Similarly, iron-modified POME sludge-based AC demonstrated an adsorption efficiency of approximately 95% [13].

Numerous studies have demonstrated the effectiveness of chemically modified activated carbon and biochar derived from agricultural and sludge-based precursors for phosphate adsorption. High removal efficiencies have been reported for MgO-modified activated carbon, reaching up to 99.1% [8-10], while Ca-modified biochar achieved adsorption efficiencies exceeding 90% [14]. Similarly, Fe/Ca co-embedded biochar exhibited removal efficiencies ranging from 85 to 98%, highlighting the synergistic role of transition metals and alkaline earth elements in enhancing adsorption performance [15]. In the case of POME sludge-derived activated carbon, physicochemical modification using calcium-based agents resulted in removal efficiencies of 90–98% [16], whereas iron-modified POME sludge-based activated carbon achieved approximately 95% removal [17].

Chemical activation remains the predominant approach for enhancing phosphate adsorption, owing to its ability to promote pore development and introduce reactive surface functional groups. MgO-biochar composites derived from empty fruit bunches (EFB) demonstrated an adsorption capacity of 9.31 mg/g, indicating strong phosphate affinity upon mineral incorporation [18]. Notably, Fe/Ca co-embedded biochar exhibited substantially higher adsorption capacities, ranging from 18.5 to 53.3 mg/g, attributable to enhanced surface complexation and electrostatic interactions facilitated by metal co-loading [19]. Further improvement was observed with calcium-enriched activation, achieving adsorption capacities as high as 97.74 mg/g [20]. Activated carbon derived from POME sludge has also shown superior phosphate uptake, with a reported adsorption capacity of 152.77 mg/g following lanthanum modification. Overall, calcium-based chemical activation (e.g., $Ca(OH)_2$) has been consistently reported to enhance adsorption performance through improved pore structure, ion exchange, and surface complexation mechanisms [14,15,21].

Despite extensive research on activated carbon derived from individual biomass or sludge-based precursors, studies exploring the combined utilisation of palm oil mill effluent (POME) sludge and empty fruit bunch (EFB) as co-precursor materials remain scarce. In particular, the synergistic effects of blending these two abundant palm oil industry by-products for activated carbon production, especially under calcium-based chemical activation, have not been systematically investigated. The interaction between the organic-rich EFB matrix and the inorganic mineral content of POME sludge may significantly influence pore development, surface chemistry, and metal dispersion, thereby affecting adsorption performance. Consequently, there is a clear knowledge gap regarding the adsorption behaviour, activation efficiency, and mechanistic pathways of Ca^{2+}-activated blended POME sludge–EFB materials. Addressing this gap is essential for advancing sustainable adsorbent development and for promoting the integrated valorisation of palm oil industry residues within a circular economy framework. Therefore, this study aims to synthesise and evaluate Ca^{2+}-impregnated blended POME sludge – EFB activated carbon for phosphate removal, with particular emphasis on adsorption performance, physicochemical characteristics and adsorption mechanism analysis.

2. Methodology

2.1 Raw Materials Preparation

The primary raw materials utilised in this study were palm oil mill effluent (POME) sludge and empty fruit bunch (EFB), both of which were obtained from palm oil processing residues in Johor, Malaysia. These materials were selected due to their abundance, high carbon content, and potential suitability as precursors for activated carbon production. The raw biomasses underwent preliminary processing to ensure homogeneity and consistency. The POME sludge and EFB were oven dried (Un110, Mermert) to remove the moisture content completely prior to pyrolysis and activation.

2.2 Pyrolysis Process

The pre-treated biomass samples were subjected to a slow pyrolysis process, which is widely recognised as an effective method for converting lignocellulosic materials into biochar with enhanced structural stability. Before pyrolysis, predetermined ratios of POME sludge and EFB were prepared to investigate the influence of biomass composition on adsorption performance. The compositions used included 100% POME sludge, 100% EFB and 60% EFB: 40% POME sludge.

Each mixture was carefully weighed and placed into ceramic boats. These were subsequently introduced into a tubular furnace (Elf 11/14B, Carbolite). Pyrolysis was conducted under an inert

nitrogen atmosphere to prevent oxidation and unwanted combustion reactions. The furnace temperature was increased gradually at a controlled heating rate until reaching 500°C, after which it was maintained for 1 hour to ensure complete thermal decomposition of volatile components. Upon completion of the heating stage, the furnace was allowed to cool naturally to room temperature under continuous nitrogen flow.

2.3 Chemical Activation Using Calcium Hydroxide

Chemical activation was employed to enhance the porosity, surface area, and surface functionality of the biochar. Calcium hydroxide ($Ca(OH)_2$ (99.9%, Sigma-Aldrich) was selected as the activating agent due to its ability to promote pore development and introduce calcium-based functional groups, which are beneficial for phosphate adsorption. The biochar samples were impregnated with $Ca(OH)_2$ at a mass ratio of 1:1. The impregnation process involved dissolving 40 g of $Ca(OH)_2$ in 150 mL of distilled water, followed by the addition of biochar into the solution. The mixture was continuously stirred and left to stand at room temperature for 1–2 hours to ensure thorough impregnation of the activating agent into the carbon matrix.

Following impregnation, the mixture was dried in an oven (Un110, Mermert) at 100°C overnight to remove excess moisture. The dried impregnated samples were then subjected to thermal activation in a furnace. Activation was conducted at 500°C, with a heating rate of 10°C/min, and maintained for 1 hour. After activation, the resulting activated carbon was washed repeatedly with distilled water to remove residual calcium compounds and impurities. Washing was continued until the filtrate reached a neutral pH. Finally, the cleaned activated carbon was oven-dried at 100°C overnight and stored in airtight containers for subsequent analyses.

2.4 Characterization Methods

To evaluate the physicochemical properties of the synthesised activated carbon, two primary characterisation techniques were employed: Scanning Electron Microscopy coupled with Energy-Dispersive X-ray Spectroscopy (SEM–EDX) and Brunauer–Emmett–Teller (BET). These methods were selected to provide complementary insights into surface morphology, pore development, and crystalline structure.

2.4.1 Scanning Electron Microscopy (SEM-EDX)

The surface morphology and elemental composition of the samples were analysed using scanning electron microscopy coupled with energy-dispersive X-ray spectroscopy (SEM–EDX). SEM analysis was conducted using a Hitachi TM3000 (Hitachi High-Tech, Japan), equipped with an AMETEK EDAX Octane series EDX detector (AMETEK Inc., USA). Providing high-resolution images that reveal surface texture, pore distribution, structural changes and elemental composition resulting from chemical activation.

Prior to analysis, the samples were cryogenically treated by freezing in liquid nitrogen for approximately 10 minutes. This step enhanced structural integrity and enabled clearer cross-sectional imaging. The samples were subsequently coated with a thin layer of platinum to improve electrical conductivity and image resolution during electron beam scanning [22]. SEM images were obtained at a magnification of x2000, allowing detailed observation of pore development and surface irregularities.

2.4.2 Brunauer- Emmett-Teller (BET)

The pore size, pore volume and average pore diameter of the samples were analysed using Brunauer-Emmett-Teller (BET) (Tristar II, Micromeritics). The BET provides insight into the properties of the materials, surface area development and pore size structure from the activation process. Approximately 0.4g of the samples was used for analysis. Adsorption-desorption isotherm was done by using nitrogen at 77k (interpreted using the BET and Barrett, Joyner, and Halenda (BJH) method) for pore size distribution and BET surface area [23].

2.5 Adsorption Method

2.5.1 Preparation of phosphate solution

A stock phosphate solution was prepared to evaluate the adsorption performance of the activated carbon samples. Sodium dihydrogen phosphate (NaH_2PO_4) (99%, Sigma-Aldrich) was used as the phosphate source due to its high solubility and stability. 1.263g of NaH_2PO_4 was weighed and dissolved in 1L of distilled water to produce a stock solution with a concentration of 1263mg/L.

2.5.2 Effect of contact time

The effect of contact time on phosphate adsorption was investigated to determine the adsorption kinetics and equilibrium behaviour of the activated carbon. Three sets of experiments were conducted using different biomass compositions 100% POME sludge, 100% EFB and 60% EFB: 40% POME sludge. For each experiment, 100g of activated carbon was added to 100 mL of the phosphate solution (200 mg/L). The mixture was agitated using a magnetic stirrer at a constant speed of 200 rpm to ensure uniform contact between the adsorbent and adsorbate.

Samples were collected at regular intervals of 3 minutes, over a total contact time of 27 minutes. At each sampling point, a small volume of sample was withdrawn using a syringe, filtered, and analysed for residual phosphate concentration using UV–Vis spectrophotometry (Vis 100, Buck Scientific). This approach allowed for the determination of adsorption behaviour as a function of time, enabling identification of equilibrium conditions and adsorption efficiency trends.

2.5.3 Effect of contaminant concentration

Phosphate solutions with initial concentrations of 100, 150, 200, 250, 300, and 350 mg/L were prepared and stirred at 200 rpm using a magnetic stirrer at an initial pH of 7 for 10 min. The data obtained was used for the isotherms study. For this procedure, the absorbance of each run was measured using a UV-Vis Spectrophotometer (Vis 100, Buck Scientific). By referencing a calibration curve that had been plotted, the measured values were used to determine the initial concentration and final concentration. The removal efficiency, expressed as the percentage of adsorption (%) and adsorption capacity (q_e), can be calculated by using Eq. (1) [24] and (2). [25], respectively:

$$Removal\ efficiency\ (\%) = \frac{c_o - c_e}{c_o} x100\% \quad (1)$$

$$q_e = \frac{(c_o - c_e)v}{m} \quad (2)$$

Where the initial concentration, mg/L (c_o), concentration of aqueous solution after adsorption, mg/L (c_e), mass of adsorbent used, g (m) and volume of the aqueous solution, L (v).

2.6 Kinetic and Isotherm Analysis

2.6.1 Interpretation of kinetic behaviors

The adsorption kinetics were analysed using pseudo-first and second order for phosphate uptake evaluation, and to determine the possible adsorption mechanism involving the interaction between phosphate ions and the activated carbon surface. The kinetic model was used to illustrate the time-dependent adsorption behaviour and to assess the suitability of each model in describing the adsorption process.

2.6.2 Adsorption isotherm

The adsorption behaviour of phosphate was evaluated using the Langmuir and the Freundlich isotherm models. The suitability of each model in describing the experimental data was assessed based on the coefficient of determination (R^2). The Langmuir and the Freundlich isotherm equations are presented in Eq. (3) [26] and (4) [27], respectively.

$$\frac{c_e}{q_e} = \frac{1}{q_m} C_e + \frac{1}{bq_m} \quad (3)$$

$$log q_e = \frac{1}{n} c_e + \log k \quad (4)$$

Where the maximum adsorption capacity, mg/g (q_m), affinity between adsorbent and phosphate, mg/L (b), the Freundlich intensity constant (n), and the Freundlich adsorption constant (log k).

3. Results and Discussion

3.1 Characterizations

The activated carbon samples were characterized using Scanning Electron Microscopy (SEM) and Brunauer–Emmett–Teller (BET) surface area analysis to evaluate their physicochemical properties. These analyses provided insights into surface morphology and pore structure aiding in understanding the adsorption mechanisms. The SEM observations presented in Figure 1 collectively confirm the presence of calcium-containing compounds, which play a critical role in phosphate adsorption. The successful incorporation of calcium derived from $Ca(OH)_2$ provides abundant reactive and adsorption sites that facilitate phosphate capture. In the presence of phosphate, the subsequent formation of calcium–phosphate phases further substantiate the proposed removal mechanism. The presence of calcium was further proved by EDX analysis, as shown in Table 1. The amount of calcium present on the surface of the AC is high. From Table 2, the size of the pores for the samples is relatively small (9.40, 10.39 and 11.2) m^2/g, resulting in a large number of pores present on the surface of the AC.

The relatively small pore size observed in the activated carbon can be attributed primarily to the nature of the precursor material and the activation conditions employed. Sludge-based precursors, such as POME sludge, are inherently rich in inorganic constituents for instance, metal oxides, silicates, and mineral ash. Which can partially inhibit extensive pore widening during carbonization and activation. The presence of these mineral phases may occupy or block developing pores, thereby limiting the formation of larger mesopores and resulting in a predominantly microporous structure. In addition, the thermal decomposition behavior of sludge differs from that of lignocellulosic

biomass, as the high ash content can reduce volatile release and restrict pore expansion during pyrolysis [16].

Beyond precursor composition, activation parameters including activating agent type, impregnation ratio, and activation temperature also play a critical role in determining pore architecture. Calcium-based activation tends to promote surface functionalization and mineral deposition rather than aggressive pore etching, particularly when compared to alkali activators such as KOH or NaOH. As a result, Ca^{2+} species may preferentially deposit within pore entrances or on internal surfaces. Contributing to a reduction in apparent pore size and specific surface area while enhancing surface chemical reactivity, as shown in comparative studies by Kundu *et al*., [28].

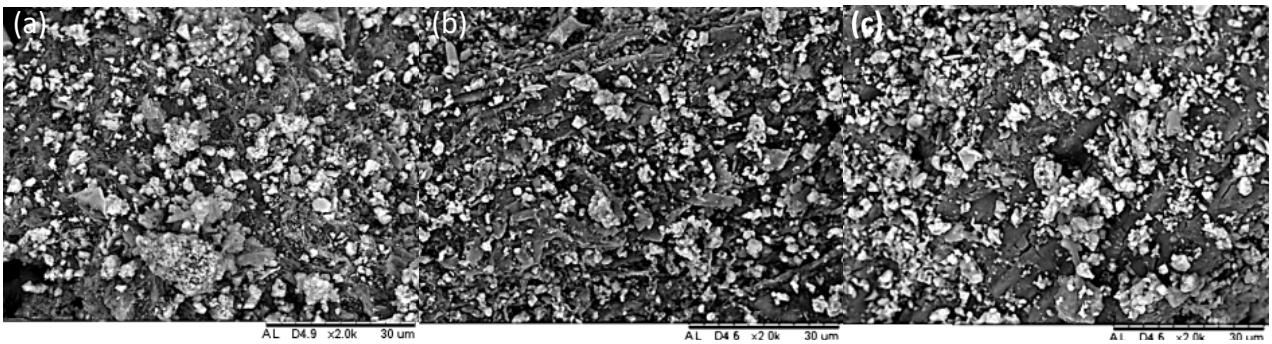

Fig. 1. The SEM images of activated carbon from three different biomass sources a)100% sludge, b) EFB 60% - 40% Sludge and c) 100% EFB

Table 1
EDX analysis on the elemental composition (wt%) of different activated carbon

	Samples		
Elements	100% EFB	EFB 60% - 40% Sludge	100% Sludge
	Weight (%)		
C	0.55	0.00	0.51
N	11.81	10.01	11.49
O	57.14	57.09	54.92
Mg	0.5	0.04	0.42
Al	0.57	0.05	0.17
Si	0.58	0.07	0.35
Ca	28.86	32.74	32.13

Table 2
Characterisation of the pore structure of activated carbon from different compositions of raw materials

	AC samples		
	100% EFB	EFB 60% - 40% Sludge	100% Sludge
BET surface Area (m^2/g)	9.40	11.2	10.39
Langmuir Area (m^2/g)	24.38	28.16	28.447
Total Pore Volume (cm^3/g)	0.0479	0.0424	0.0535
Average Pore Diameter (A)	204.053	151.252	206.214
t-Plot Micropore Area	11.397	13.064	13.199

3.2 Adsorption Performance

Batch adsorption experiments were performed to evaluate the performance of the activated carbons under varying contaminant concentrations. To isolate the effect of initial phosphate concentration, the contact time was fixed at 10 minutes, while the adsorbent dosage (0.1 g), agitation

speed (200 rpm), and phosphate solution volume (100 mL) were maintained constant. The initial phosphate concentrations investigated ranged from 100 to 350 mg/L, specifically 100, 150, 200, 250, 300, and 350 mg/L, to assess their influence on phosphate adsorption behavior. Figures 2 and 3 illustrate the effect of increasing phosphate concentration on the removal efficiency and equilibrium adsorption capacity (q_e) of the activated carbons.

As illustrated in Figure 2 (a), an increase in the initial contaminant concentration leads to a corresponding rise in the adsorption capacity for all three activated carbon samples. At the highest tested phosphate concentration of 350 mg/L, the maximum adsorption capacity was achieved by AC–EFB (60%)–sludge (40%), reaching 347.55 mg/g, followed closely by AC–sludge (100%) at 347.05 mg/g and AC–EFB (100%) at 347.02 mg/g. These results indicate that higher phosphate concentrations provide a greater driving force for mass transfer, thereby enhancing adsorption uptake.

In contrast, Figure 2 (b) demonstrates that the percentage removal of phosphate was highest at the lowest initial concentration of 100 mg/L and gradually declined as the phosphate concentration increased. Among the samples, AC–EFB (100%) exhibited superior removal efficiency at elevated concentrations. At 350 mg/L, this sample achieved the highest phosphate removal efficiency of 99.15%, compared with 97.45% for AC–EFB (60%)–sludge (40%) and 97.02% for AC–sludge (100%). Overall, all activated carbons displayed consistently high removal performance, with only marginal differences observed across the concentration range investigated. The observed trends indicate that while adsorption capacity increases with increasing contaminant concentration, removal efficiency exhibits an inverse relationship with initial phosphate concentration. This behaviour is consistent with adsorption theory and aligns with the findings reported by Ilham *et al*., [29], who investigated phosphate adsorption using biomass-derived activated carbon under batch adsorption conditions. Their study similarly demonstrated higher adsorption performance at lower phosphate concentrations, supporting the conclusion that reduced initial contaminant levels favor more efficient phosphate adsorption in the present system. In addition, the results of this study also reported higher/ on par performance of developed activated carbon with literatures reported that the adsorption performance of phosphate was in the range of 98.4 to 99.4% by using Pangium edule shells as precursor and activation via NaOH chemical, followed by pyrolysis under nitrogen atmosphere.

Despite the relatively small pore size, calcium-impregnated activated carbon demonstrates effective phosphate adsorption, indicating that adsorption is governed not solely by physical pore filling but also by strong chemical interactions at the adsorbent surface. Calcium species introduced during activation can form positively charged surface sites, which enhance electrostatic attraction toward negatively charged phosphate species (e.g. $H_2PO_4^-$ and HPO_4^{2-}) under neutral pH conditions. This mechanism allows phosphate adsorption to occur predominantly at or near the external surface and pore mouths, reducing dependence on deep pore diffusion [21].

Furthermore, calcium impregnation facilitates ligand exchange and surface complexation reactions, whereby phosphate ions replace hydroxyl or carbonate groups coordinated to calcium sites [15]. In some cases, the formation of calcium–phosphate precipitates or inner-sphere complexes on the carbon surface has been reported, contributing to high adsorption capacity even in materials with limited mesoporosity [20]. These chemisorption-dominated pathways are particularly advantageous for phosphate removal, as phosphate uptake relies more on reactive surface sites than on high surface area alone.

The results suggest that while sludge-derived activated carbon may exhibit smaller pore sizes due to precursor mineral content and calcium-based activation, the incorporation of Ca^{2+} species compensates for these structural limitations by introducing highly effective adsorption sites. This highlights the importance of surface chemistry over pore size distribution in the design of activated

carbon for phosphate removal and supports the suitability of calcium-modified sludge-based materials for targeted nutrient adsorption applications [30].

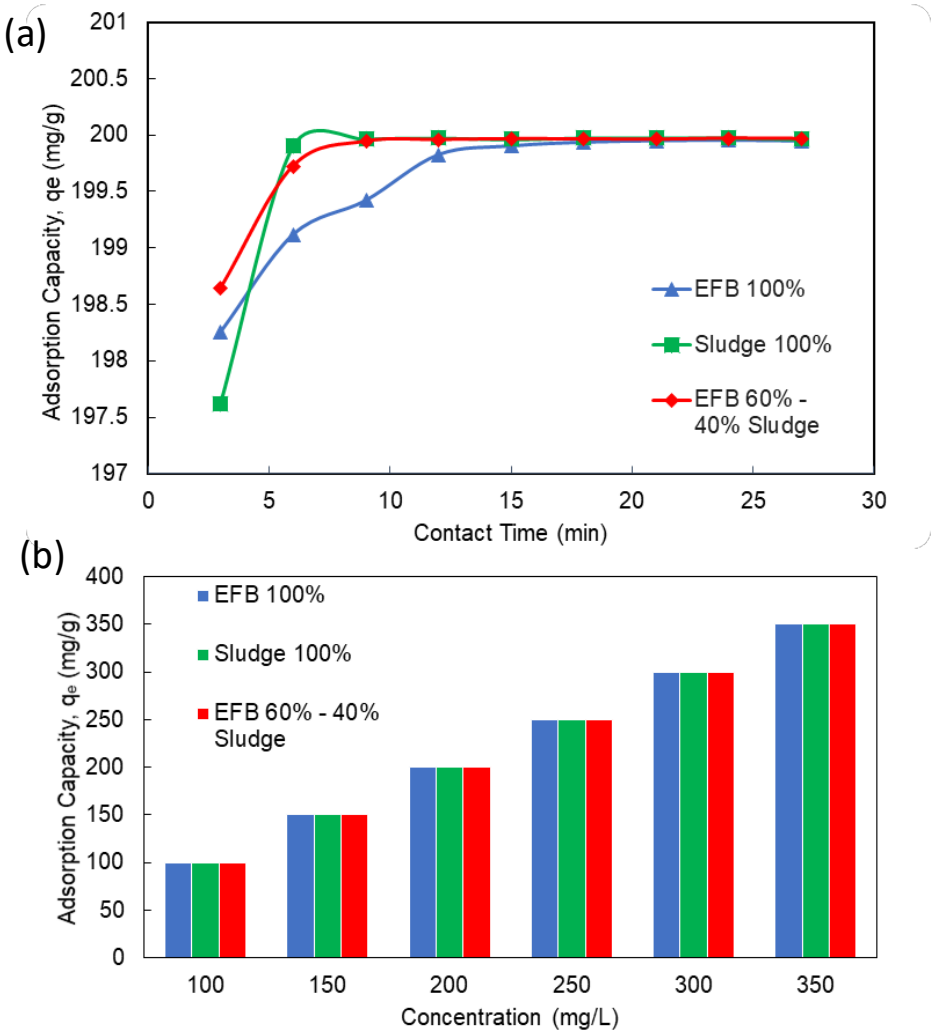

Fig. 2. (a) Adsorption capacity (mg/g) with varying contact time (min) and (b) Adsorption capacity (mg/g) with varying concentration of contaminant (mg/L)

3.3 Adsorption Isotherms

The adsorption behavior of phosphate ions onto $Ca(OH)_2$-activated carbons derived from different biomass compositions was evaluated using the Langmuir and the Freundlich isotherm models to elucidate adsorption capacity, surface characteristics, and governing mechanisms. The derived isotherm parameters (Table 2) provide important insight into how precursor composition influences adsorption performance and surface heterogeneity.

The Langmuir isotherm analysis revealed relatively high maximum adsorption capacities (q_{max}) for all adsorbents, indicating that $Ca(OH)_2$ activation effectively generates reactive adsorption sites regardless of precursor composition. The activated carbon derived from 100% EFB exhibited the highest q_{max} value (332.652 mg/g), followed closely by the sludge-based carbon (317.328 mg/g) and the EFB–sludge composite (312.841 mg/g). The narrow range of q_{max} values suggests that phosphate uptake is governed by similar adsorption mechanisms across all samples, likely dominated by

calcium-mediated interactions rather than solely by textural properties. The marginally higher q_{max} observed for the EFB-derived carbon may be attributed to its more developed carbon matrix and lower mineral content, which facilitates greater accessibility of Ca^{2+}-based adsorption sites and more uniform monolayer coverage [31].

The Langmuir affinity constant (b) further differentiates the adsorption behavior among the samples. A positive b value obtained for the 100% EFB-derived activated carbon indicates favorable adsorption and a strong affinity between phosphate ions and the adsorbent surface. In contrast, negative b values observed for sludge-containing carbons suggest deviations from ideal Langmuir behavior, likely arising from surface heterogeneity, mineral interference, or non-uniform energy distribution of adsorption sites. The presence of inorganic constituents in sludge may disrupt the formation of a homogeneous monolayer and introduce competing interactions, thereby violating the assumptions of the Langmuir model. Nevertheless, the high correlation coefficients ($R^2 > 0.98$) obtained for all samples indicate strong mathematical fitting, implying that while the Langmuir model describes the overall adsorption trend well, its physical assumptions may not be fully applicable, particularly for sludge-containing materials.

In contrast, the Freundlich isotherm provides insight into adsorption on heterogeneous surfaces and multilayer adsorption processes. The Freundlich capacity constant (Kf) was highest for the EFB–sludge composite (393.236), followed by the 100% sludge (339.361) and 100% EFB (326.193) samples. This trend highlights the beneficial role of sludge incorporation in enhancing adsorption capacity through increased surface heterogeneity and the introduction of diverse functional groups and mineral-associated active sites. The synergistic combination of organic carbon from EFB and inorganic constituents from sludge may create a broader distribution of adsorption energies, facilitating phosphate uptake across multiple surface domains.

Furthermore, the Freundlich exponent (n) exceeded unity for all samples, confirming favorable adsorption conditions. The highest n value observed for the 100% sludge-derived activated carbon ($n = 8.835$) suggests a highly heterogeneous surface with strong adsorption intensity, consistent with the complex surface chemistry imparted by mineral-rich sludge. The slightly lower n values for the EFB and EFB–sludge samples still indicate favorable adsorption but reflect comparatively more uniform surface characteristics.

Despite its mechanistic relevance, the Freundlich model exhibited lower correlation coefficients than the Langmuir model (Table 3), with the highest R^2 (0.893) obtained for the 100% EFB-derived activated carbon and reduced fitting quality for sludge-containing samples. This reduced fitting performance suggests that multilayer adsorption alone cannot fully explain the adsorption behavior, particularly in systems where multiple mechanisms coexist. The deviations from ideal Freundlich behavior indicate contributions from pore-filling effects, surface precipitation, electrostatic attraction, and chemisorption mediated by calcium species. These findings are consistent with previous studies reporting that phosphate adsorption onto metal-modified carbons often involves a combination of physical and chemical interactions rather than a single dominant mechanism [32].

Overall, the combined isotherm analysis demonstrates that while the Langmuir model effectively captures the high adsorption capacity and favorable affinity of the EFB-derived activated carbon, the Freundlich model more accurately reflects the heterogeneous and multilayer adsorption behavior introduced by sludge incorporation. The divergence between statistical fitting and physical interpretation underscores the complexity of phosphate adsorption onto $Ca(OH)_2$-activated carbons and highlights that no single isotherm model can comprehensively describe the adsorption process. These results emphasize the importance of considering both precursor composition and surface chemistry in the design of calcium-activated carbon materials for efficient phosphate removal [33].

Table 3
Comparison of Langmuir and the Freundlich isotherm constants for phosphate adsorption

Adsorbent AC-Ca(OH)2	Langmuir Isotherm			Freundlich Isotherm		
	q_m	b	R^2	n	Kf	R^2
100% EFB	332.652	41.390	0.982	7.556	326.193	0.893
100% Sludge	317.328	0.000138	0.991	8.835	339.361	0.718
EFB 60% - 40% Sludge	312.841	0.00014	0.992	7.357	393.236	0.737

4. Conclusions

This study successfully demonstrated the feasibility of AC produced from a combination of EFB and sludge using calcium species for activation. The physicochemical characterization confirmed that all prepared activated carbons possessed comparable textural and surface properties, with BET surface areas of 9.404 m²/g for 100% EFB, 11.200 m²/g for the EFB–POME sludge blend, and 10.393 m²/g for 100% sludge, indicating that blending did not adversely affect pore development. SEM–EDX analysis verified the successful incorporation of calcium species on the carbon surfaces, evidenced by distinct bright regions, which contributed to enhanced phosphate affinity. Batch adsorption experiments revealed consistently high phosphate removal performance for all samples, achieving a maximum adsorption capacity of 347.55 mg/g at an initial phosphate concentration of 350 mg/L. Isotherm analysis further indicated favorable adsorption behavior, with the Langmuir model providing excellent representation of the adsorption process ($R^2 > 0.98$), and the highest monolayer adsorption capacity observed for 100% EFB (q_{max} = 332.652 mg/g), while the EFB–POME sludge composite exhibited the highest Freundlich constant (Kf = 393.236), reflecting greater surface heterogeneity. Collectively, these findings confirm that both single and blended EFB–POME sludge precursors can be effectively valorized into high-performance calcium-activated carbons for phosphate removal, supporting sustainable waste-to-resource conversion and circular economy implementation in wastewater treatment.

Acknowledgement
The authors acknowledge the financial support from the Ministry of Higher Education (MOHE) under the Fundamental Research Grant Scheme (FRGS) (FRGS/1/2024/TK05/UTM/02/9) and Universiti Teknologi Malaysia for funding under Universiti Teknologi Malaysia Encouragement Grant (Q.J130000.3846.31J75).

References

[1] Basiron, Yusof. "Palm oil and its global supply and demand prospects." *Oil palm industry economic journal* 2, no. 1 (2002): 1-10.
[2] Koh, H. L., W. K. Tan, S. Y. Teh, and C. J. Tay. "Water quality simulation for rehabilitation of a eutrophic lake in Selangor, Malaysia." In *IOP Conference Series: Earth and Environmental Science*, vol. 380, no. 1, p. 012006. IOP Publishing, 2019.doi: 10.1088/1755-1315/380/1/012006.
[3] Salgado, Jorge, Carl D. Sayer, Stephen J. Brooks, Thomas A. Davidson, Ben Goldsmith, Ian R. Patmore, Ambroise G. Baker, and Beth Okamura. "Eutrophication homogenizes shallow lake macrophyte assemblages over space and time." *Ecosphere* 9, no. 9 (2018): e02406. doi: 10.1002/ecs2.2406.

[4] Sedyaaw, P., V. R. Bhatkar, and A. N. Sawant. "A review on effects of eutrophication in aquatic ecosystem." *International Journal of Development Research* 14, no. 4 (2024): 65362-65369. https://doi.org/10.37118/ijdr.28143.04.2024

[5] Ouakouak, A. K., and L. Youcef. "Phosphates removal by activated carbon." *Sensor Letters* 14, no. 6 (2016): 600-605. doi: 10.1166/sl.2016.3664.

[6] Nadagouda, Mallikarjuna N., Gaiven Varshney, Vikas Varshney, and Charifa A. Hejase. "Recent advances in technologies for phosphate removal and recovery: A review." *ACS environmental Au* 4, no. 6 (2024): 271-291. doi: 10.1021/acsenvironau.3c00069.

[7] J. Andas, M. L. A. Rahman, and M. S. M. Yahya, "Preparation and Characterization of Activated Carbon from Palm Kernel Shell," *IOP Conf. Ser. Mater. Sci. Eng.*, vol. 226, no. 1, 2017, doi: 10.1088/1757-899X/226/1/012156.

[8] Baffour-Awuah, E., S. A. Akinlabi, T. C. Jen, S. Hassan, I. P. Okokpujie, and F. Ishola. "Characteristics of palm kernel shell and palm kernel shell-polymer composites: a review." In *IOP Conference Series: Materials Science and Engineering*, vol. 1107, no. 1, p. 012090. IOP Publishing, 2021. doi: 10.1088/1757-899x/1107/1/012090.

[9] Luka, Y., B. K. Highina, and A. Zubairu. "The promising precursors for development of activated carbon: Agricultural waste materials-A review." *Journal Impact Factor* 3 (2018): 46. doi: 10.7324/ijasre.2018.32615.

[10] Abdul Rani, Noor Hidayu, Nor Fadilah Mohamad, Sharmeela Matali, and Sharifah Aishah Syed A. Kadir. "Preparation and characterization of activated carbon made from oil palm empty fruit bunch." *Key Engineering Materials* 594 (2014): 44-48. doi: 10.4028/www.scientific.net/KEM.594-595.44.

[11] Lei, W. A. N. G., L. I. Luyao, Y. A. N. G. Zhenglong, Y. A. N. G. Zongkun, W. A. N. G. Minyan, C. H. E. N. Hao, S. H. E. N. Cheng, and Z. H. A. N. G. Jin. "Microstructure of calcium-iron modified biochar and its effect on phosphate adsorption from aqueous solution." *Journal of Zhejiang A&F University* 43, no. 1 (2026): 142-152. doi: 10.11833/j.issn.2095-0756.20250128.

[12] Zeng, Shufang, Xin Lan, Peng Liu, Zhongxing Zhang, Xi Cheng, Nuchao Xu, and Huilin Yin. "Removal of Phosphate from Water by Iron/Calcium Oxide-Modified Biochar: Removal Mechanisms and Adsorption Modeling." *Water* 16, no. 22 (2024): 3245. doi: 10.3390/w16223245.

[13] Boki, Keito, Seiki Tanada, Tamotstu Miyoshi, Ryoji Yamasaki, Nobuhiro Ohtani, and Takamichi Tamura. "Phosphate removal by adsorption to activated carbon." *Nippon Eiseigaku Zasshi (Japanese Journal of Hygiene)* 42, no. 3 (1987): 710-720. doi: 10.1265/jjh.42.710.

[14] Xu, Cancan, Rui Liu, Qi Tang, Yifan Hou, Lvjun Chen, and Quanxi Wang. "Adsorption removal of phosphate from rural domestic sewage by Ca-modified biochar derived from waste eggshell and sawdust." *Water* 15, no. 17 (2023): 3087. doi: 10.3390/ma16175873.

[15] Zeng, Shufang, Xin Lan, Peng Liu, Zhongxing Zhang, Xi Cheng, Nuchao Xu, and Huilin Yin. "Removal of Phosphate from Water by Iron/Calcium Oxide-Modified Biochar: Removal Mechanisms and Adsorption Modeling." *Water* 16, no. 22 (2024): 3245. doi: 10.3390/w16223245.

[16] Zhou, Yujun, Jiamin Gao, Xuran Yang, Hao Ni, Junwen Qi, Zhigao Zhu, Yue Yang, Di Fang, Lixiang Zhou, and Jiansheng Li. "Recent progress in sludge-derived biochar and its role in wastewater purification." *Sustainability* 16, no. 12 (2024): 5012. doi: 10.3390/su16125012.

[17] Inyinbor, A. A., F. A. Adekola, and Gabriel Ademola Olatunji. "Kinetics, isotherms and thermodynamic modeling of liquid phase adsorption of Rhodamine B dye onto Raphia hookerie fruit epicarp." *Water Resources and Industry* 15 (2016): 14-27. doi: 10.1016/j.wri.2016.06.001.

[18] Wahba, Shimaa M., Kate Scott, and Julia K. Steinberger. "Analyzing Egypt's water footprint based on trade balance and expenditure inequality." *Journal of Cleaner Production* 198 (2018): 1526-1535. doi: 10.1016/j.jclepro.2018.06.266.

[19] Amalina, Farah, Abdul Syukor Abd Razak, Santhana Krishnan, Haspina Sulaiman, A. W. Zularisam, and Mohd Nasrullah. "Biochar production techniques utilizing biomass waste-derived materials and environmental applications–A review." *Journal of Hazardous Materials Advances* 7 (2022): 100134. doi: 10.1016/j.hazadv.2022.100134.

[20] Cheng, Fulong, Yinian Wang, Yuting Fan, Dan Huang, Jie Pan, and Wei Li. "Optimized Ca-Al-La modified biochar with rapid and efficient phosphate removal performance and excellent pH stability." *Arabian Journal of Chemistry* 16, no. 8 (2023): 104880. doi: 10.1016/j.arabjc.2023.104880.

[21] Erasga, Eden S., Christine Joy D. Dimarucut, John Kyla M. Larino, and Bren Julius T. Pablo. "Phosphate Adsorption from Aqueous Solution Using Activated Carbon from Saba Banana Peels Impregnated with Ca2+." *Chemical Engineering Transactions* 113 (2024): 271-276.doi: 10.3303/CET24113046.

[22] "Cryo-Electron Microscopy Train for advanced research." [Online]. Available: www.myscope.training

[23] Sanda Mamane, O., R. Souley Moussa, M. N. Amadou Kiari, A. R. Chaibou Yacouba, M. Siragi Dounounou Boukari, A. Sanda Bawa, O. Mahaman Sani, M. M. Malam Alma, and I. Natatou. "Determination of the specific surface areas

of activated carbons produced from local lignocellulosic biomass (Niger) using the BET, Langmuir and BJH methods." *J. Mater. Environ. Sci., 16 (10), 1893-1907* (2025).

[24] Yusop, Mohamad Firdaus Mohamad, Erniza Mohd Johan Jaya, and Mohd Azmier Ahmad. "Single-stage microwave assisted coconut shell based activated carbon for removal of Zn (II) ions from aqueous solution–Optimization and batch studies." *Arabian Journal of Chemistry* 15, no. 8 (2022): 104011. doi: 10.1016/j.arabjc.2022.104011.

[25] Benallou, M. Benzekri, N. Douara, M. A. Chemrak, Z. Mekibes, N. Benderdouche, and B. Bestani. "Elimination of Malachite Green on granular activated carbon prepared from olive stones in discontinuous and continuous modes." *Algerian Journal of Environmental Science and Technology* 7, no. 1 (2021).

[26] Sulaiman, Nurul Syuhada, Mohd Hazim Mohamad Amini, Mohammed Danish, Othman Sulaiman, and Rokiah Hashim. "Kinetics, thermodynamics, and isotherms of methylene blue adsorption study onto cassava stem activated carbon." *Water* 13, no. 20 (2021): 2936. doi: https:// doi.org/10.3390/w13202936.

[27] J. Sankari, P. Kalaivani, D. Sitrarasu, R. Pagutharivalan, and N. Kannan, "Adsorption Study With Different Eco-Friendly Activated Carbons For The Removal Of Basic Dye From Aqueous Solution," *Int. J. Environ. Sci.*, vol. 11, no. 5s, pp. 323–336, 2025. doi: 10.64252/4gd42g36.

[28] Kundu, Shreyase, Tasmina Khandaker, Md Al-Amin Mia Anik, Md Kamrul Hasan, Palash Kumar Dhar, Sagar Kumar Dutta, M. Abdul Latif, and Muhammad Sarwar Hossain. "A comprehensive review of enhanced CO 2 capture using activated carbon derived from biomass feedstock." *RSC advances* 14, no. 40 (2024): 29693-29736. doi: 10.1039/d4ra04537h.

[29] Ilham, Rachmannu, Fataty Rahmah, Nurul Said, Mohamad Budiono, and Suprapto Suprapto. "Optimization of Phosphate Adsorption Using Activated Carbon Derived from." *Journal of Renewable Materials* 12, no. 11 (2024): 1895. doi: 10.32604/jrm.2024.055602.

[30] Zhuo, Guang-Hui, Dong-Xin Xue, Long-Fei Huang, Qi Wang, Guangcan Zhu, and Chu-Ya Wang. "Adsorption of phosphates on a novel eggshell Ca-modified anaerobic sludge-based biochar: Adsorption performance and mechanism." *Plos one* 20, no. 11 (2025): e0337183. doi: 10.1371/journal.pone.0337183.

[31] Mo, Jingjing, Qian Li, Xiaojie Sun, Hongxia Zhang, Meiyan Xing, Bin Dong, and Hongxiang Zhu. "Capacity and mechanisms of phosphate adsorption on lanthanum-modified dewatered sludge-based biochar." *Water* 16, no. 3 (2024): 418. doi: 10.3390/w16030418.

[32] Biswas, Bijoy, Tawsif Rahman, Manish Sakhakarmy, Hossein Jahromi, Mohamed Eisa, Jonas Baltrusaitis, Jasmeet Lamba, Allen Torbert, and Sushil Adhikari. "Phosphorus adsorption using chemical and metal chloride activated biochars: Isotherms, kinetics and mechanism study." *Heliyon* 9, no. 9 (2023). doi: 10.1016/j.heliyon.2023.e19830.

[33] Areerob, Yonrapach, Dinh Cung Tien Nguyen, Biswas Md Rokon Dowla, Hyuk Kim, Je-Woo Cha, and Won-Chun Oh. "Synthesis and characterization of calcium derivative combined with high-surface-area activated carbon composites for fine toxic gas removal." *Journal of the Korean Ceramic Society* 55, no. 5 (2018): 473-479. doi: 10.4191/kcers.2018.55.5.02.